De novo expression of connexin hemichannels in denervated fast skeletal muscles leads to atrophy

Luis A. Cea[a,b,1], Bruno A. Cisterna[a], Carlos Puebla[a,b], Marina Frank[c], Xavier F. Figueroa[a], Christopher Cardozo[d,e], Klaus Willecke[c], Ramón Latorre[b,1], and Juan C. Sáez[a,b,1]

[a]Departamento de Fisiología, Pontificia Universidad Católica de Chile, Santiago 6513677, Chile; [b]Centro Interdisciplinario de Neurociencias de Valparaíso, Universidad de Valparaíso, Valparaíso 2366103, Chile; [c]Life and Medical Sciences Institute, Division of Molecular Genetics, University of Bonn, 53115 Bonn, Germany; [d]Center of Excellence for the Medical Consequences of Spinal Cord Injury, James J. Peters Veterans Affairs Hospitals Medical Center, Bronx, NY 10468; and [e]Department of Medicine, Mount Sinai School of Medicine, New York, NY 10468

Contributed by Ramón Latorre, August 14, 2013 (sent for review June 25, 2013)

Denervation of skeletal muscles induces atrophy, preceded by changes in sarcolemma permeability of causes not yet completely understood. Here, we show that denervation-induced Evans blue dye uptake in vivo of fast, but not slow, myofibers was acutely inhibited by connexin (Cx) hemichannel/pannexin1 (Panx1) channel and purinergic ionotropic $P2X_7$ receptor ($P2X_7R$) blockers. Denervated myofibers showed up-regulation of Panx1 and de novo expression of Cx39, Cx43, and Cx45 hemichannels as well as $P2X_7Rs$ and transient receptor potential subfamily V, member 2, channels, all of which are permeable to small molecules. The sarcolemma of freshly isolated WT myofibers from denervated muscles also showed high hemichannel-mediated permeability that was slightly reduced by blockade of Panx1 channels or the lack of Panx1 expression, but was completely inhibited by Cx hemichannel or $P2X_7R$ blockers, as well as by degradation of extracellular ATP. However, inhibition of transient receptor potential subfamily V, member 2, channels had no significant effect on membrane permeability. Moreover, activation of the transcription factor NFκB and higher mRNA levels of proinflammatory cytokines (TNF-α and IL-1β) were found in denervated WT but not Cx43/Cx45-deficient muscles. The atrophy observed after 7 d of denervation was drastically reduced in Cx43/Cx45-deficient but not Panx1-deficient muscles. Therefore, expression of Cx hemichannels and $P2X_7R$ promotes a feed-forward mechanism activated by extracellular ATP, most likely released through hemichannels, that activates the inflammasome. Consequently, Cx hemichannels are potential targets for new therapeutic agents to prevent or reduce muscle atrophy induced by denervation of diverse etiologies.

connexons | membrane leakage | purinergic receptors | phosphorylated p65 | inflammation

Denervated skeletal muscles undergo a change in membrane permeability along with a progressive array of metabolic, structural, and functional changes that lead to atrophy (1). For example, at approximately 7 d after denervation, rodent skeletal muscles show a decrease in intracellular K^+ concentration (2) and an increase in intracellular Na^+ concentration (1) and total calcium content (1). In addition, contraction of denervated skeletal muscle depends on extracellular Ca^{2+} as early as 6 d after denervation (3). A possible explanation for this latter result is that denervation induces the expression of the cardiac Ca^{2+} permeable dihydropyridine receptor isoform (4). However, this protein is only expressed from day 25 of denervation. Therefore, the Ca^{2+}-dependency of denervated muscles for a single contraction remains unexplained (4). The increase in dihydropyridine receptors Cav1.1 and ryanodine receptor complex has also been proposed to contribute to the increase in free Ca^{2+} concentration (5), but the denervation-induced reduction in membrane potential (V_m) is not sufficient to activate these channels (6). The changes in intracellular Na^+ and K^+ concentrations and V_m reduction of denervated myofibers might be explained by a deficiency in Na^+/K^+-dependent ATPase pump activity, but ouabain still induces a ~10% reduction in V_m in denervated myofibers (7). Consequently, the transmembrane electrochemical changes induced by denervation are, at present, not fully explained. An alternative mechanism could be the de novo expression of nonselective cation channels, which, to our knowledge, has not been reported. Investigation of this possibility was the main goal of the present work.

To date, treatments with several compounds have only partially reduced the development of atrophy (8). However, substantial reduction of myofiber atrophy has been obtained upon muscle-specific inhibition of NF-κB through expression of IκB-α superrepressor (1) or genetic deletion of either of two muscle-specific E3 ligases, atrogin-1 or muscle ring finger-1 (MurF1) (1). However, the sequence of events that initiates muscle atrophy and the relevance of most changes induced by denervation remain uncertain.

Here, we demonstrated that denervated fast skeletal muscles express de novo the monovalent cation and Ca^{2+} permeable channels connexins (Cxs) 39, 43, and 45, purinergic ionotropic $P2X_7$ receptors ($P2X_7Rs$), as well as transient receptor potential, subfamily V, member 2 (TRPV2), channels, and show an up-regulation of pannexin1 (Panx1). The relevance of functional Cx hemichannels and $P2X_7Rs$ in denervation-induced permeabilization of the sarcolemma was also demonstrated. In addition, denervation was found to induce an inflammatory state of myofibers associated with muscular atrophy, and both responses were greatly

Significance

In this paper two biological findings are described and explain several muscle changes induced by denervation: (*i*) the sarcolemma of fast myofibers are permeabilized to small molecules such as Evans blue via connexin (Cx) hemichannels and (*ii*) the absence of Cx43/Cx45 hemichannels greatly attenuates the inflammasome activation and muscle atrophy. The first finding explains the activation of proteolysis in denervated muscles. The second demonstrates that muscle inflammation can occur without inflammatory cell infiltration, offering an explanation how denervated muscles can alter other tissues. These findings unveil therapeutic targets to reduce atrophy in diverse clinical conditions. Because Cx hemichannels are permeable to Evans blue, the use of this dye as tracer of cell damage should be reevaluated in different systems.

Author contributions: L.A.C., X.F.F., C.C., K.W., R.L., and J.C.S. designed research; L.A.C., B.A.C., C.P., and M.F. performed research; L.A.C. and M.F. contributed new reagents/analytic tools; L.A.C., B.A.C., and C.P. analyzed data; and L.A.C., C.P., X.F.F., C.C., K.W., R.L., and J.C.S. wrote the paper.

The authors declare no conflict of interest.

[1]To whom correspondence may be addressed. E-mail: lacea@uc.cl, ramon.latorre@uv.cl, or jsaez@bio.puc.cl.

This article contains supporting information online at www.pnas.org/lookup/suppl/doi:10.1073/pnas.1312331110/-/DCSupplemental.

reduced in Cx43/Cx45-deficient myofibers, revealing the importance of Cx hemichannels in this pathological condition.

Results

ATP-Activated Cx43/Cx45 Hemichannels and $P2X_7$ Receptors Permeabilize Denervated Fast Myofibers. Because the sarcolemma permeability of denervated myofibers is likely to be altered, we evaluated it in vivo through the use of Evans blue dye (EB^{4-}; 960.8 Da). The dye was administered to rats 7 d after unilateral hindlimb denervation, and cross-sections of control (innervated contralateral) and denervated extensor digitorum longus (EDL) muscles (fast muscles) were obtained. In samples of denervated muscles, EB^{4-} fluorescence was located in the interstitium as well as inside the myofibers, whereas, in samples of control muscles, the EB^{4-} fluorescence was restricted to the interstitial space (Fig. 1 *A* and *B*). In EDL muscles, fluorescence intensity of intracellular EB^{4-} increased progressively from 3 d to 7 d and 21 d after denervation. In contrast to denervated EDL muscles, myofibers of denervated rat soleus muscles (slow muscle) did not show intracellular EB^{4-} staining at 3, 7, or 21 d after denervation.

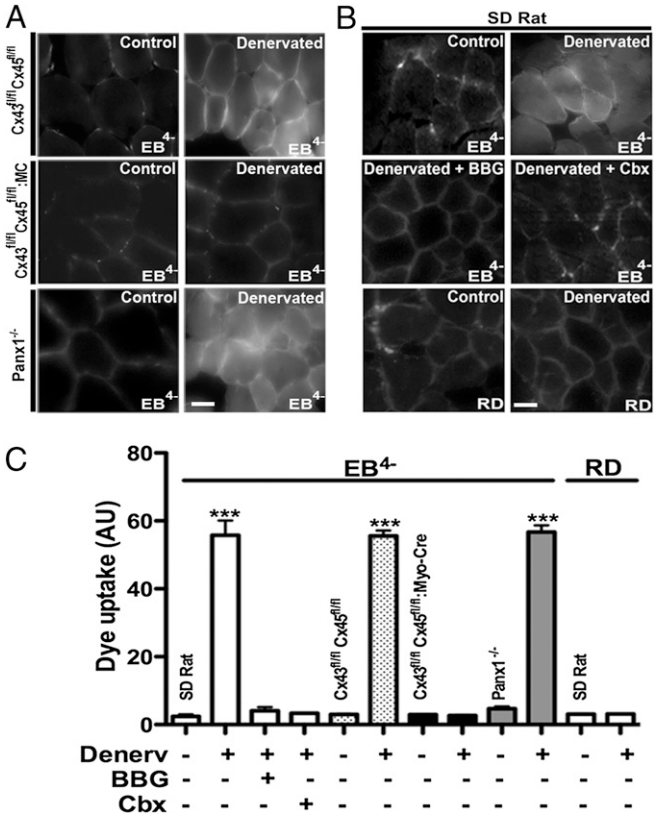

Fig. 1. Denervated (Denerv) but not innervated myofibers of fast muscles show intracellular EB^{4-} staining prevented by inhibition of $P2X_7$Rs or hemichannels. Rat EDL muscles (fast) and mouse TA muscles (fast) were used at day 7 after denervation. Mice were $Cx43^{fl/fl}Cx45^{fl/fl}$ (dotted bars), $Cx43^{fl/fl}Cx45^{fl/fl}$:Myo-Cre (black bars), and $Panx1^{-/-}$ (gray bars). Animals were injected with EB^{4-} (80 mg/kg) or RD (800 mg/kg). Data on rat muscles correspond to white bars. (*A*) Photomicrographs illustrate the findings in mouse TA muscles. (Scale bar: 20 μm.) (*B*) Intracellular EB^{4-} fluorescence was evident in rat denervated EDL muscles, but was not observed in muscles of rats pretreated (20 min before the EB^{4-} injection) with Cbx (80 mg/kg), a Cx hemichannel/Panx1 channel and $P2X_7$R blocker, or BBG (45 mg/kg), a $P2X_7$R and Panx1 inhibitor. Similarly, RD was found only in the extracellular space of denervated rat EDL muscles. Photomicrographs illustrate the findings in rat EDL muscles. (Scale bar: 20 μm.) (*C*) Graph illustrates quantification of fluorescence intensity in at least 10 sections per animal obtained in four independent experiments for each condition (***$P < 0.001$, $n = 4$ animals per group).

To test whether membrane channels might be involved in altered membrane permeability, we evaluated the effects of channel inhibitors on entry of EB^{4-} into denervated myofibers. EB^{4-} was found only in the interstitium of denervated muscles of rats treated 20 min before EB^{4-} administration with brilliant blue G (BBG), a $P2X_7$R and Panx1 inhibitor, or carbenoxolone (Cbx), a Cx hemichannel/Panx1 channel and $P2X_7$R blocker (9) (Fig. 1*B*). These findings suggested that the intracellular accumulation EB^{4-} of denervated myofibers did not result from membrane damage, but rather was a consequence of uptake through a membrane pathway composed of functional $P2X_7$Rs and Cx hemichannels/Panx1 channels. Further demonstration that intracellular EB^{4-} found in denervated EDL myofibers was a result of increased membrane permeability instead of membrane damage was obtained in rats injected with rhodamine dextran (RD; 10 kDa), which has a molecular weight well greater than the size exclusion of any physiological membrane pore. RD was detected only in the interstitium in denervated EDL muscles at 7 d, as well as in contralateral nondenervated EDL muscles (Fig. 1*B*).

To further extend the pharmacologic data supporting the possible involvement of Panx channels and Cx hemichannels in the permeabilization of denervated myofibers, permeability of denervated myofibers was then evaluated in $Panx1^{-/-}$ mice and muscle-specific Cx43/Cx45-deficient mice. After 7 d of denervation, tibialis anterior (TA; fast muscle) myofibers of $Panx1^{-/-}$ mice showed intracellular EB^{4-} fluorescence, and this was absent in the contralateral muscle, in which EB^{4-} was found only in the interstitium (Fig. 1*A*). Likewise, denervated but not innervated TA myofibers of $Cx43^{flox/flox}/Cx45^{flox/flox}$ mice (control mice; Fig. 1 *A* and *C*) or WT mice showed prominent EB^{4-} staining in their interior. In contrast, denervated as well as innervated TA myofibers of $Cx43^{fl/fl}/Cx45^{fl/fl}$:Myo-Cre mice (skeletal muscle-specific Cx43/Cx45-deficient mice) did not show intracellular EB^{4-} fluorescence (Fig. 1).

Normal skeletal myofibers express Panx1 channels in T tubules but they do not express Cxs (1, 10) (Fig. 2*A*). Accordingly, Cx39, Cx43, and Cx45 were not detected by immunofluorescence staining in control EDL (rat) and TA (mouse) muscles (Fig. 2*A*). However, the three Cxs known to be expressed during development or regeneration (Cxs 39, 43, and 45) (11–13) were detected in denervated EDL muscles (Fig. 2*A* and Fig. S1). Moreover, immunofluorescence revealed that denervated muscles also express $P2X_7$Rs and TRPV2 channels and showed up-regulation of Panx1 (Fig. 2*A*). In agreement with their possible role in permeabilization of denervated myofibers, immunoreactivity of all six proteins was detected mainly in the sarcolemma (Fig. 2*A*). Similar results were obtained in gastrocnemius muscles of rats with spinal cord transection (Fig. S2). Moreover, control fast muscles did not express functional gap junction channels (Fig. S3). Levels of all proteins studied were unchanged in slow denervated muscles (Fig. S4).

The relative importance of possible molecular elements involved in the sarcolemma permeabilization of denervated fast muscles was studied in acutely dissociated myofibers with selective blockers of $P2X_7$R, TRPV2 channels, and Cx hemichannel or Panx channels. In these experiments, EB^{4-} was replaced by ethidium (Etd^+), which allows real-time measurement of cell membrane permeability changes via Cx hemichannels or Panx1 channels (14, 15).

Myofibers of denervated flexor digitorum brevis (FDB, a fast muscle) muscles of rats showed approximately threefold higher Etd^+ uptake (Fig. 2*B*, *Inset*, encircled fluorescent nuclei) than control muscles (Fig. 2*B*), which was completely blocked by La^{3+}, a Cx hemichannel and P2XR blocker (16) (Fig. 2 *B* and *C*). In control rat myofibers, the Etd^+ uptake rate was not significantly reduced by La^{3+}; A740003, a selective $P2X_7$R blocker (17); or Cbx, a Cx hemichannel/Panx1 channel and $P2X_7$R blocker (9). However, the Etd^+ uptake rate of denervated myofibers treated

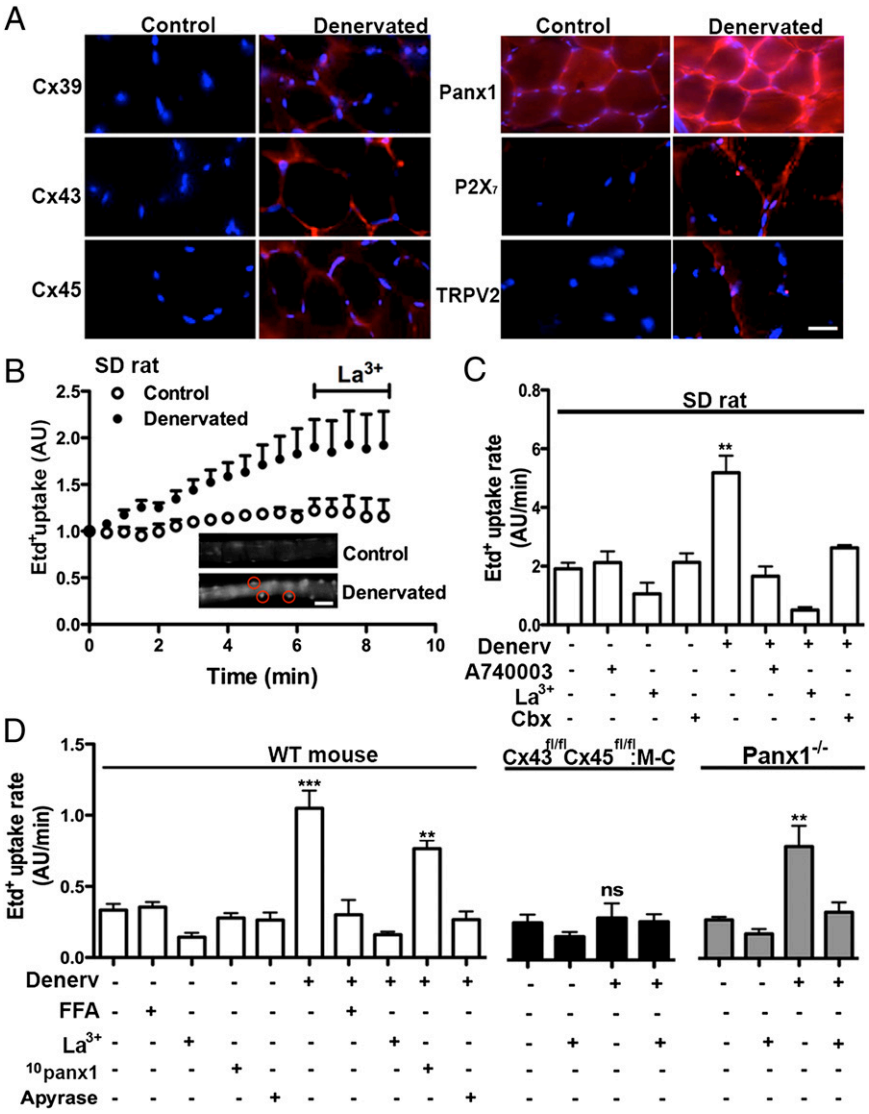

Fig. 2. The sarcolemma permeability of denervated fast myofibers is increased mainly via a P2X7R- and connexin (Cx) hemichannel-dependent mechanism. Acutely dissociated myofibers of denervated (Denerv) and contralateral Sprague Dawley rat (SD rat, *A* and *B*) or mouse (*C*) *flexor digitorum brevis* (FDB, fast) muscles were used. At day 7 after denervation, the Etd^+ uptake of myofibers was evaluated. (*A*) After 7 d of denervation, the distribution of Cx39, Cx43, Cx45, Panx1 P2X7R and TRPV2 reactivity was evaluated by immunofluorescence assays in cross-sections of rat EDL muscle fibers. All proteins studied were mainly detected in the sarcolemma of the myofibers. ($n = 3$). (Scale bar: 20 μm.) (*B*) Representative record of fluorescence intensity (i.e., Etd^+ uptake) over time of nuclei of denervated (closed circles) and control myofibers (open circles). The progressive Etd^+ uptake of rat denervated myofibers was inhibited by La^{3+}, a P2XR and Cx hemichannel blocker. (*Insets*) Regions of interest around nuclei (red) of control (*Upper*) and denervated (*Lower*) myofibers incubated for 6 min in saline solution containing Etd^+. (Scale bar: 20 μm.) (*C*) Etd^+ uptake rates of control and denervated rat myofibers in the absence or presence of La3+, A740003 (10 M, a selective inhibitor of $P2X_7Rs$), and Cbx (200 M; a $P2X_7R$ and Cx hemichannel/Panx1 channel inhibitor). All inhibitors were applied acutely as in *B*. (*D*) Etd^+ uptake rate of control and denervated myofibers of FDB muscles from WT, $Cx43^{fl/fl}Cx45^{fl/fl}$:Myo-Cre and $Panx1^{-/-}$ mice. Effects of 100 M flufenamic acid (FFA; Cx hemichannel inhibitor), 200 M La^{3+}, 200 M ^{10}panx1 (Panx1 channel blocker), and 2 units/mL apyrase (ATP hydrolase): each treatment is denoted below each bar with a plus sign. A minimum of 20 fibers were analyzed per condition ($n = 4$ animals per group; $^{***}P < 0.001$ vs. all conditions except with ^{10}panx1, which was not significant vs. WT myofibers; $^{**}P < 0.01$ vs. all conditions in $Panx1^{-/-}$ mice; ns, not significant). Values shown as mean SEM.

with La^{3+}, A740003, or Cbx was indistinguishable from that of control myofibers treated with the same agents (Fig. 2*C*). In support of the role of Cx hemichannels in denervation-induced sarcolemma permeabilization, myofibers of denervated FDB muscles obtained from Cx43/Cx45-deficient mice ($Cx43^{fl/fl}$ $Cx45^{fl/fl}$:Myo-Cre) did not show a significant increase of Etd^+ uptake compared with innervated WT myofibers (Fig. 2*D*). However, denervated myofibers of WT (Fig. 2*C*) or $Cx43^{fl/fl}$ $Cx45^{fl/fl}$ mice showed similar, high Etd^+ uptake that was blocked by La^{3+} or flufenamic acid, inhibitors of Cx hemichannels but not Panx1 channels (9); 200 μM ^{10}Panx1, a selective Panx1 channel blocker (9); or 20 min preincubation with apyrase, an ATP hydrolase (Fig. 2*D*). Moreover, the Etd^+ uptake of denervated Panx1-deficient FDB myofibers was comparable to that of denervated WT myofibers treated with ^{10}Panx1 and was also drastically reduced by La^{3+} (Fig. 2*D*). To test the possible involvement of TRPV2 channels, denervated WT myofibers were acutely treated with tranilast, a TRPV2 channel blocker (18), but the Etd^+ uptake remained as in untreated denervated WT myofibers.

To test if Cx hemichannels are permeable to EB^{4-}, HeLa cells transfected with Cx39, Cx43, or Cx45 were bathed with divalent cation-free solution to increase their open probability (14) in the presence of 1 mM EB^{4-}. All transfected but not parental cells showed EB^{4-} uptake (Fig. S5 *A*, *a*–*d*) that was prevented by 200 μM La^{3+} or 100 μM Cbx (Fig. S5*B*). However, HeLa-Panx1 cells treated with bisindolylmaleimide, a PKC inhibitor that increases the open probability of Panx1 HCs, did not show EB^{4-} uptake (Fig. S5 *A*, *e*). HeLa-TRPV2 cells treated with 2-aminoethyl diphenylborinate (2-APB), a potent TRPV2 channel activator (19), also did not show EB^{4-} uptake (Fig. S5 *A*, *f*). However, the intracellular Ca^{2+} signal showed a rapid increase in HeLa-TRPV2 but not in HeLa-parental cells (Fig. S5*C*), indicating that TRPV2 channels were activated by 2-APB causing Ca^{2+} inflow.

Denervation of Fast Skeletal Muscles Induces Activation of the Inflammasome. Denervation induces an early and transient increase in muscle levels of TNF-α and IL-1β (20), which are products of inflammasome activation (21). Because activation of the nuclear factor kappa-light-chain-enhancer of activated B cells (NF-κB), a transcription factor, induces muscle atrophy (1), we decided to evaluate levels of the phosphorylated form of p65 (P-p65), an active subunit of NF-κB (22). At 7 d after denervation, P-p65 reactivity was increased in the cytoplasm (Fig. 3*A*, red) and in nuclei (DAPI-stained) in denervated (Fig. 3*A*, white arrows) but not innervated myofibers of TA muscles of control ($Cx43^{fl/fl}Cx45^{fl/fl}$) mice. In addition, the P-p65 reactivity in denervated myofibers of Cx43/Cx45-deficient TA muscles ($Cx43^{fl/fl}$ $Cx45^{fl/fl}$:Myo-Cre mice) was comparable to that of innervated

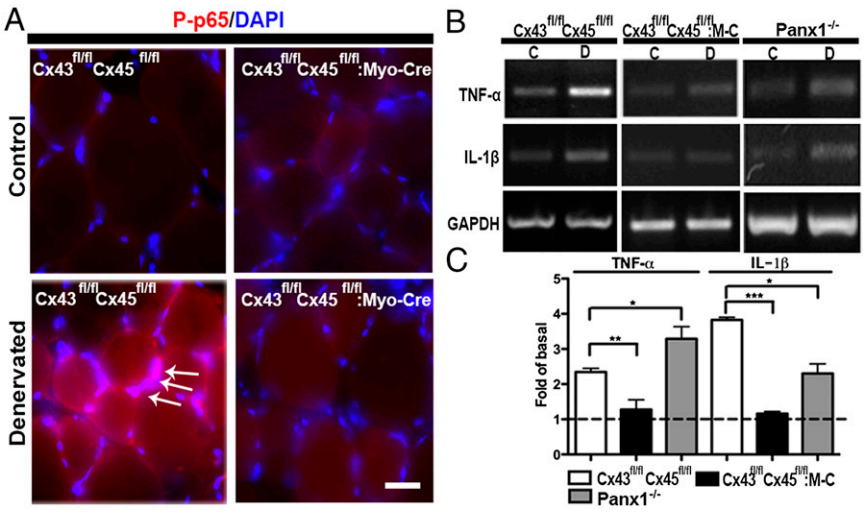

Fig. 3. Denervation-induced inflammation in TA muscle. The presence of P-p65 (red) transcription factor was evaluated by immunofluorescence in fixed cryosections of control and denervated (7 d) TA (fast) muscles of $Cx43^{fl/fl}Cx45^{fl/fl}$ and $Cx43^{fl/fl}Cx45^{fl/fl}$:Myo-Cre mice. Nuclei were stained with DAPI (blue). (*A*) P-p65 was detected in the cytoplasm (red) and in the nuclei (arrows denote fuchsia nuclei in merged images) in denervated TA of $Cx43^{fl/fl}Cx45^{fl/fl}$ mice but not in Cx43/Cx45-deficient ($Cx43^{fl/fl}Cx45^{fl/fl}$:Myo-Cre) muscles or innervated $Cx43^{fl/fl}Cx45^{fl/fl}$ or $Cx43^{fl/fl}Cx45^{fl/fl}$:Myo-Cre muscles. (Scale bar: 50 μm.) (*B*) mRNA levels of TNF-α and IL-1β were evaluated by RT-PCR, and levels of both mRNAs were increased in denervated muscles of $Cx43^{fl/fl}Cx45^{fl/fl}$ and $Panx1^{-/-}$ but not $Cx43^{fl/fl}Cx45^{fl/fl}$:Myo-Cre mice ($Cx43^{fl/fl}Cx45^{fl/fl}$:M-C). (*C*) quantification of blots shown in *B*, as fold of basal value (not denervated). Values presented as mean ± SEM ($n = 3$ animals per group; $^*P < 0.05$ and $^{***}P < 0.001$).

control myofibers or innervated Cx43/Cx45-deficient myofibers (Fig. 3*A*). Because activated NF-κB promotes the expression of proinflammatory cytokines, including TNF-α and IL-1β, levels of mRNA of these cytokines were evaluated by RT-PCR. Relative levels of both mRNAs were significantly higher in denervated TA muscles of $Cx43^{fl/fl}Cx45^{fl/fl}$ mice (Fig. 3*B*), whereas, in denervated muscles of Cx43/Cx45-deficient mice, they remained similar to those for innervated controls ($Cx43^{fl/fl}Cx45^{fl/fl}$) or Cx43/Cx45-deficient muscles (Fig. 3 *B* and *C*).

Absence of Cx43 and Cx45 but Not Panx1 Drastically Reduces Denervation-Induced Muscular Atrophy. Control and denervated TA muscles of Cx43/Cx45-deficient and control mice were obtained at day 7 of denervation, and the cross-sectional area (CSA) of myofibers was evaluated and taken as a measurement of muscular atrophy. Myofibers of denervated muscles showed a drastic reduction in CSA (~82% of control CSA) compared with myofibers of innervated control and Cx43/Cx45-deficient muscles (Fig. 4). However, the myofiber CSA in TA muscles of $Cx43^{fl/fl}Cx45^{fl/fl}$:Myo-Cre mice was reduced only by approximately 30% relative to control muscles (Fig. 4). Notably, these myofibers still expressed Cx39 and TRPV2 reactivity and showed up-regulation of Panx1 but did not express detectable reactivity of $P2X_7Rs$ (Fig. S6). Moreover, the absence of Panx1 did not prevent denervation-induced myofiber atrophy in TA muscles; the reduction in CSA of myofibers of $Panx1^{-/-}$ mice was similar to that of denervated control or $Cx43^{fl/fl}Cx45^{fl/fl}$ muscles (Fig. 4*B*). Myofibers of denervated $Panx1^{-/-}$ TA muscles showed high reactivity for Cx39, Cx43, Cx45, $P2X_7R$, and TRPV2 channel (Fig. S6).

Discussion

Here, we demonstrated that denervated fast skeletal myofibers show de novo expression of Cxs (39, 43, and 45), $P2X_7Rs$, and TRPV2 channels and up-regulation of Panx1. They do not express functional gap junctions, but they present functional hemichannels and $P2X_7Rs$, which permeabilize the sarcolemma to small molecules, resulting in increased extracellular ATP concentration. The absence of Cx43 and Cx45 in myofibers is sufficient to drastically attenuate the denervation-induced activation of the inflammasome and atrophy, suggesting that increased membrane permeability through expression of hemichannels and increased expression of channels is part of a feed-forward mechanism for activation of the inflammasome and muscle atrophy. Although no changes in membrane permeability or expression of the proteins studied were found in slow myofibers, it remains to be determined if such changes occur after much longer periods of time as occurs for other features of denervated slow muscles (23).

We found that denervated fast myofibers, which are atrophic but not damaged or dead (24), show intracellular EB^{4-} staining after systemic administration but they do not incorporate RD (excluded by membrane channels), and the intracellular staining with EB^{4-} was completely prevented by BBG or Cbx, indicating the integrity of the plasma membrane and the involvement of P2X receptors and Cx hemichannels/Panx1 channels as diffusional pathways for EB^{4-} uptake. A relevant role for Panx1 can be ruled out because denervated myofibers of $Panx1^{-/-}$ mice showed EB^{4-} uptake comparable to that of WT denervated myofibers, and HeLa-Panx1 cells treated with bisindolylmaleimide to open Panx1 channels did not show EB^{4-} uptake. Moreover, cells without Panx1 channel expression do not show ATP-induced Etd^+ uptake (15), indicating that $P2X_7Rs$ may not be the membrane pathway for dye uptake in denervated myofibers. In addition, EB^{4-} has been found to inhibit P2X receptors (25). Therefore, the only known membrane pathways for EB^{4-} uptake in denervated myofibers are Cx hemichannels.

Consistent with this interpretation, myofibers of denervated muscle from Cx43/Cx45-deficient mice did not show EB^{4-} or Etd^+ uptake. Increased EB^{4-} uptake by denervated WT mouse myofibers was completely blocked by La^{3+} and Cbx and more importantly by flufenamic acid, a rather selective Cx hemichannel blocker (9). Moreover, HeLa cells transfected with Cxs (39, 43, or 45) but not HeLa-parental cells, showed EB^{4-} uptake that was completely inhibited by Cx hemichannel blockers (La^{3+} and Cbx). In addition, the possible role of TRPV2 channels in Etd^+ uptake by denervated myofibers can be ruled because tranilast, an inhibitor of TRPV2 channels, had no effect, and 2-APB, an activator of TRPV2 channels, promoted a rapid Ca^{2+} influx, but did not induce EB^{4-} uptake in HeLa-TRPV2 cells. Accordingly, our evidence indicates that denervated myofibers show de novo expression of Cx hemichannels that permeabilize the sarcolemma to EB^{4-} and Etd^+.

In innervated normal myofibers, electrical stimulation induces ATP release via Panx1 channels, which also allow Etd^+ uptake (10). Here, we found that extracellular apyrase blocks the elevated membrane permeability (Etd^+ uptake) of denervated WT myofibers under resting conditions, revealing that they spontaneously release ATP and that ATP promotes the increase in membrane permeability. As Panx1 channels and Cx hemichannels are permeable to ATP (26), and both were found to be highly expressed in the sarcolemma of denervated WT myofibers, they are likely the sarcolemmal pathway for ATP release. However, permeabilization via Panx1 channels might be less prominent than that via Cx hemichannels because inhibition of

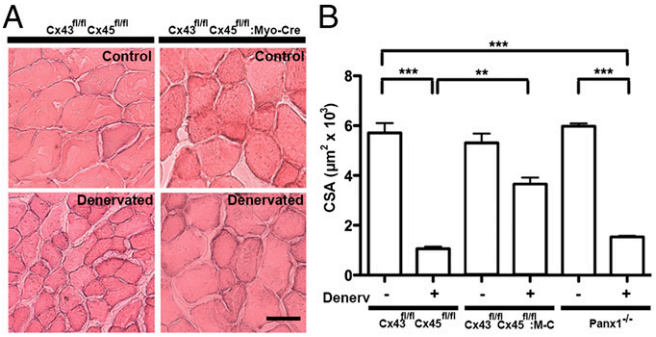

Fig. 4. The absence of Cx43 and Cx45 but not of Panx1 greatly reduces denervation-induced muscular atrophy. TA muscles of $Cx43^{fl/fl}Cx45^{fl/fl}$, $Cx43^{fl/fl}Cx45^{fl/fl}$:Myo-Cre, or $Panx1^{-/-}$ mice were denervated. At day 7 after denervation, cryo–cross-sections were obtained from TA muscles and stained with H&E. (*A*) A significant reduction (~82%) in CSA of myofibers was found in denervated TA muscles from $Cx43^{fl/fl}Cx45^{fl/fl}$ and $Panx1^{-/-}$ mice. The reduction in CSA induced by denervation was reduced (~30%) in muscles of $Cx43^{fl/fl}Cx45^{fl/fl}$:Myo-Cre mice. (Scale bar: 50 μm.) (*B*) Quantification of at least 10 sections of each muscle. M-C, Myo-Cre ($n = 4$ independent experiments for each group; $^{**}P < 0.01$ and $^{***}P < 0.001$).

Panx1 channels with ^{10}Panx1 or the absence of Panx1 in myofibers of $Panx^{-/-}$ mice caused a similar partial reduction (<30%) in Etd^+ uptake, whereas inhibition of Cx hemichannels with flufenamic acid or the absence of Cx43/Cx45 completely abrogated the Etd^+ uptake. Additionally, our findings do not exclude a role for calcium homeostasis modulator 1 (CALHM1), which recently has been described as an ATP channel (27).

In agreement with the role of extracellular ATP in permeabilization of the sarcolemma of denervated myofibers, we found that inhibition of $P2X_7Rs$ both in vivo (i.e., effect of BBG on EB^{4-} uptake) and in vitro (i.e., effect of A740003 on Etd^+ uptake) blocked dye uptake completely. The findings described here strongly suggest the establishment of a feed-forward mechanism wherein ATP released through Cx hemichannels activates $P2X_7Rs$ in an orchestrated way, permeabilizes the sarcolemma, and increases the intracellular Ca^{2+} levels, thereby sustaining membrane depolarization and enhancing membrane permeability, and initiating and/or enhancing activation of the inflammasome. In support of this interpretation is the finding that the membrane channels studied that affect the sarcolemma permeability, specifically, $P2X_7Rs$, Cx hemichannels, and Panx1 channels, are known to be permeable to Ca^{2+}, and their open probability is increased by a reduction in extracellular Ca^{2+} concentration that might occur as a result of the Ca^{2+} inflow via the same channels (28). Moreover, the increase in intracellular free Ca^{2+} concentration favors the insertion of Cx hemichannels into the sarcolemma (28) and activation of Cx hemichannels and Panx1 channels (26) through which ATP is released; this ATP release would further activate $P2X_7Rs$ maintaining the feed-forward mechanism "on."

De novo expression of Cx43 in fast muscles might first result from denervation-induced reduction of miR-206 (29), which is known to repress the expression of Cx43 (30). A second mechanism that might induce the Cx expression could be mediated by proinflammatory cytokines released by denervated myofibers showing activation of the inflammasome, because TNF-α and IL-1β promote expression of Cx hemichannels in fast myofibers (1) and denervated muscles express high levels of TNF-α and IL-1β as soon as 24 h after denervation (20); this up-regulation may continue for several more days, as we found high mRNA levels of TNF-α and IL-1β in 7-d denervated muscles. However, the initial signals up-regulating expression of Cx hemichannels seems to occur upstream of proinflammatory cytokine expression because we found that levels of cytokine mRNAs did not increase in denervated Cx43/Cx45-deficient muscles. Thus, the proinflammatory cytokines might constitute a second feed forward mechanism that amplifies the muscle response to denervation.

Because denervated Cx43/Cx45-deficient muscles did not show a significant increase in $P2X_7Rs$, it is conceivable that the regulation of $P2X_7R$ expression is downstream of these two Cxs. Moreover, the expression of Cx39, Panx1, and TRPV2 might be under the control of independent factor(s) similar to the one(s) that regulate(s) the expression of Cx43/Cx45 because denervated muscles of Cx43/Cx45-deficient mice still showed high levels of these proteins. Whether the expression of all six proteins studied is under the control of a Ca^{2+} signaling pathway remains to be determined.

The intracellular Ca^{2+} signal generated by opening Cx43, Cx45, $P2X_7$, and TRPV2, which form Ca^{2+} permeable channels (26, 28, 31), could activate the NLRP3 inflammasome complex, leading to production of proinflammatory cytokines (21). Upstream of the inflammasome, activation of the transcription factor NF-κB frequently occurs, and its inactivation prevents muscle atrophy induced by various conditions, including denervation (1). Similarly, we found that loss of Cx43/Cx45 expression drastically prevents the activation of NF-κB and up-regulation of TNF-α and IL-1β mRNAs, indicating the relevance of Cx hemichannels as upstream activators of NF-κB and the inflammasome. The involvement of $P2X_7Rs$ and Panx1 channels in activation of the inflammasome complex in neurons and astrocytes has been proposed (32). Here, we found that $P2X_7Rs$ in conjunction with Cx43/Cx45 hemichannels but not Panx1 channels are determinants for activation of the muscle inflammasome after denervation, suggesting that different membrane components might be involved in activation of the inflammasome of different cell types.

Denervated myofibers express a program that leads to degeneration of skeletal myofibers associated with an increase in total intracellular calcium (1). In the present study, denervated myofibers were found to express de novo Ca^{2+} permeable channels ($P2X_7R$, TRPV2, Panx1, Cx43 hemichannels), which could serve as pathways for Ca^{2+} inflow (26, 33), and some of them also participate in the ATP outflow. Consequently, the increase of extracellular ATP concentration appears to activate purinergic receptors (P2X and P2Y) expressed by myofibers (33–35), thereby increasing the free $[Ca^{2+}]_i$. Moreover, Cx43 hemichannels are permeable to NAD^+, which, besides activating $P2X_7Rs$ expressed in denervated fast myofibers, can also be cycled by extracellular CD38 and then cross the cell membrane via Cx43 hemichannels, where it activates ryanodine receptors (36), further contributing to increase the free $[Ca^{2+}]_i$. Our findings suggest that all of these pathways converge to activate protein degradation pathways (37) that characterize the cachexic state.

Because denervation is the outcome of damage to motor neurons of diverse causes including traumatic, degenerative, or genetic injury to nerves, or to lack of neurotransmission of genetic or acquired origin (1), a similar mechanism as the one described here could explain muscle atrophy in diverse neuropathological conditions. Therefore, Cx hemichannels might be therapeutic targets to drastically reduce the resulting muscle degeneration.

Materials and Methods

Reagents and detailed methods are described in *SI Materials and Methods*.

Animals. All studies were approved by the Institutional Bioethics Committee (Protocol 176) of the Pontificia Universidad Católica de Chile. All efforts were made to minimize animal suffering, to reduce the number of animals used, and to use alternatives to in vivo techniques if available. Male Sprague–Dawley rats (~300 g) and C57/Bl6, $Cx43^{fl/fl}Cx45^{fl/fl}$, and male $Cx43^{fl/fl}Cx45^{fl/fl}$:Myo-Cre mice were used. The latter were skeletal muscle-deficient for Cx43 and Cx45 generated from breeding $Cx43^{fl/fl}$ mice (38) and $Cx45^{fl/fl}$ mice (39) with Myo-Cre mice, which express Cre recombinase under the control of a myogenin promoter and the MEF2C enhancer (40).

PHYSIOLOGY

EB^{4-} Uptake In Vivo. Animals with unilateral hindlimb denervation were injected i.p. 6 h before euthanasia with EB^{4-} (80 mg/kg) dissolved in sterile saline solution. To inhibit the in vivo EB^{4-} uptake by myofibers, Cbx (80 mg/kg), a Cx hemichannel/Panx1 channel and $P2X_7R$ blocker, or BBG (45 mg/kg), a $P2X_7R$ and Panx1 inhibitor, was administered (i.p.) 20 min before the EB^{4-} injection. To test for defects in sarcolemma integrity, RD (10 kDa, 800 mg/kg of body weight) was injected i.p. 6 h before euthanasia. Then, animals were killed, muscles were dissected and fast-frozen in isopentane precooled in liquid nitrogen, and EB^{4-} and RD fluorescence intensity (λ excitation, 545 nm; λ emission, 595 nm) was quantified on cross-sections in intracellular regions by using a conventional Nikon Eclipse Ti fluorescent microscope (EB^{4-} λ excitation, 545 nm; λ emission, 595 nm).

CSA Measurements. The CSA of skeletal muscle fibers observed in cross-sections fixed with 4% (wt/vol) paraformaldehyde and stained with H&E was evaluated by using offline analyses by ImageJ software (National Institutes of Health).

Statistical Analyses. Results are presented as mean ± SE. Two populations were compared by using the logarithm of ratio followed by Student *t* test. For multiple comparisons with a single control, a nonparametric one-way ANOVA followed by the Bonferroni test was used. Analyses were carried out by using GraphPad software. *P* values <0.05 were considered statistically significant.

ACKNOWLEDGMENTS. This work was partially supported by grants Fondo Nacional de Desarrollo Científico y Tecnológico 1111033 (to L.A.C. and J.C.S.) and 1100850 (to X.F.F.), Comisión Nacional de Ciencia y Tecnología-Deutscher Akademischer Austausch Dienst 2009-187 (to K.W. and J.C.S.), German Research Foundation Wi270/33-1, Sonderforschungsbereich 645 B2 (to K.W.), Fondo de Fomento al Desarrollo Científico y Tecnológico D07I1086 (to J.C.S.), Chilean Science Millennium Institute P09-022-F (to R.L. and J.C.S.), and Department of Veterans Affairs Rehabilitation Research and Development Service B9212C and B4616 (to C.C.). Data from this work were presented by L.A.C. as partial fulfillment of the requirements to obtain a PhD in Physiological Sciences at Pontificia Universidad Católica de Chile and as part of the PhD thesis of B.A.C.

1. Cea LA, et al. (2012) Connexin- and pannexin-based channels in normal skeletal muscles and their possible role in muscle atrophy. *J Membr Biol* 245(8):423–436.
2. Leader JP, et al. (1984) Cellular ions in intact and denervated muscles of the rat. *J Membr Biol* 81(1):19–27.
3. Kirby AC, Lindley BD, Picken JR (1973) Calcium dependence of potassium contractures in denervated frog muscle. *Am J Physiol* 225(1):166–170.
4. Péréon Y, Sorrentino V, Dettbarn C, Noireaud J, Palade P (1997) Dihydropyridine receptor and ryanodine receptor gene expression in long-term denervated rat muscles. *Biochem Biophys Res Commun* 240(3):612–617.
5. Kraner SD, et al. (2011) Upregulation of the CaV 1.1-ryanodine receptor complex in a rat model of critical illness myopathy. *Am J Physiol Regul Integr Comp Physiol* 300(6):R1384–R1391.
6. Beam KG, Knudson CM (1988) Calcium currents in embryonic and neonatal mammalian skeletal muscle. *J Gen Physiol* 91(6):781–798.
7. Clausen T, Kjeldsen K, Nørgaard A (1983) Effects of denervation on sodium, potassium and [^{3}H]ouabain binding in muscles of normal and potassium-depleted rats. *J Physiol* 345:123–134.
8. Servais S, Letexier D, Favier R, Duchamp C, Desplanches D (2007) Prevention of unloading-induced atrophy by vitamin E supplementation: links between oxidative stress and soleus muscle proteolysis? *Free Radic Biol Med* 42(5):627–635.
9. D'hondt C, Ponsaerts R, De Smedt H, Bultynck G, Himpens B (2009) Pannexins, distant relatives of the connexin family with specific cellular functions? *Bioessays* 31(9): 953–974.
10. Riquelme MA, et al. (2013) The ATP required for potentiation of skeletal muscle contraction is released via pannexin hemichannels. *Neuropharmacology*, 10.1016/j.neuropharm.2013.03.022.
11. Araya R, Riquelme MA, Brandan E, Sáez JC (2004) The formation of skeletal muscle myotubes requires functional membrane receptors activated by extracellular ATP. *Brain Res Brain Res Rev* 47(1-3):174–188.
12. Araya R, et al. (2005) Expression of connexins during differentiation and regeneration of skeletal muscle: Functional relevance of connexin43. *J Cell Sci* 118(pt 1):27–37.
13. von Maltzahn J, Wulf V, Matern G, Willecke K (2011) Connexin39 deficient mice display accelerated myogenesis and regeneration of skeletal muscle. *Exp Cell Res* 317(8):1169–1178.
14. Contreras JE, et al. (2002) Metabolic inhibition induces opening of unapposed connexin 43 gap junction hemichannels and reduces gap junctional communication in cortical astrocytes in culture. *Proc Natl Acad Sci USA* 99(1):495–500.
15. Pelegrin P, Surprenant A (2006) Pannexin-1 mediates large pore formation and interleukin-1beta release by the ATP-gated $P2X_7$ receptor. *EMBO J* 25(21):5071–5082.
16. Nakazawa K, Liu M, Inoue K, Ohno Y (1997) Potent inhibition by trivalent cations of ATP-gated channels. *Eur J Pharmacol* 325(2-3):237–243.
17. Honore P, et al. (2006) A-740003 [N-(1-[(cyanoimino)(5-quinolinylamino) methyl] amino-2,2-dimethylpropyl)-2-(3,4-dimethoxyphenyl)acetamide], a novel and selective P2X7 receptor antagonist, dose-dependently reduces neuropathic pain in the rat. *J Pharmacol Exp Ther* 319(3):1376–1385.
18. Hisanaga E, et al. (2009) Regulation of calcium-permeable TRPV2 channel by insulin in pancreatic beta-cells. *Diabetes* 58(1):174–184.
19. Neeper MP, et al. (2007) Activation properties of heterologously expressed mammalian TRPV2: Evidence for species dependence. *J Biol Chem* 282(21):15894–15902.
20. Hanwei H, Zhao H (2010) FYN-dependent muscle-immune interaction after sciatic nerve injury. *Muscle Nerve* 42(1):70–77.
21. Murakami T, et al. (2012) Critical role for calcium mobilization in activation of the NLRP3 inflammasome. *Proc Natl Acad Sci USA* 109(28):11282–11287.
22. Jang MK, et al. (2001) Ca^{2+}/calmodulin-dependent protein kinase IV stimulates nuclear factor-kappa B transactivation via phosphorylation of the p65 subunit. *J Biol Chem* 276(23):20005–20010.
23. Braun TP, et al. (2011) Central nervous system inflammation induces muscle atrophy via activation of the hypothalamic-pituitary-adrenal axis. *J Exp Med* 208(12): 2449–2463.
24. Bruusgaard JC, Gundersen K (2008) In vivo time-lapse microscopy reveals no loss of murine myonuclei during weeks of muscle atrophy. *J Clin Invest* 118(4):1450–1457.
25. Bültmann R, Starke K (1993) Evans blue blocks P2X-purinoceptors in rat vas deferens. *Naunyn Schmiedebergs Arch Pharmacol* 348(6):684–687.
26. Baroja-Mazo A, Barberà-Cremades M, Pelegrín P (2013) The participation of plasma membrane hemichannels to purinergic signaling. *Biochim Biophys Acta* 1828(1): 79–93.
27. Taruno A, et al. (2013) CALHM1 ion channel mediates purinergic neurotransmission of sweet, bitter and umami tastes. *Nature* 495(7440):223–226.
28. Schalper KA, et al. (2008) Connexin hemichannel composition determines the FGF-1-induced membrane permeability and free $[Ca^{2+}]_i$ responses. *Mol Biol Cell* 19(8): 3501–3513.
29. Hsieh CH, et al. (2011) Altered expression of the microRNAS and their potential target genes in the soleus muscle after peripheral denervation and reinnervation in rats. *J Trauma* 70(2):472–480.
30. Anderson C, Catoe H, Werner R (2006) MIR-206 regulates connexin43 expression during skeletal muscle development. *Nucleic Acids Res* 34(20):5863–5871.
31. O'Neil RG, Heller S (2005) The mechanosensitive nature of TRPV channels. *Pflugers Arch* 451(1):193–203.
32. Silverman WR, et al. (2009) The pannexin 1 channel activates the inflammasome in neurons and astrocytes. *J Biol Chem* 284(27):18143–18151.
33. Sluyter R, Shemon AN, Barden JA, Wiley JS (2004) Extracellular ATP increases cation fluxes in human erythrocytes by activation of the $P2X_7$ receptor. *J Biol Chem* 279(43): 44749–44755.
34. Chen Y, Li GW, Wang C, Gu Y, Huang LY (2005) Mechanisms underlying enhanced P2X receptor-mediated responses in the neuropathic pain state. *Pain* 119(1-3):38–48.
35. Voss AA (2009) Extracellular ATP inhibits chloride channels in mature mammalian skeletal muscle by activating P2Y1 receptors. *J Physiol* 587(pt 23):5739–5752.
36. Song EK, et al. (2011) Connexin-43 hemichannels mediate cyclic ADP-ribose generation and its Ca^{2+}-mobilizing activity by NAD^+/cyclic ADP-ribose transport. *J Biol Chem* 286(52):44480–44490.
37. Yazaki M, Kashiwagi K, Aritake K, Urade Y, Fujimori K (2012) Rapid degradation of cyclooxygenase-1 and hematopoietic prostaglandin D synthase through ubiquitin-proteasome system in response to intracellular calcium level. *Mol Biol Cell* 23(1): 12–21.
38. Theis M, et al. (2001) Endothelium-specific replacement of the connexin43 coding region by a lacZ reporter gene. *Genesis* 29(1):1–13.
39. Maxeiner S, et al. (2005) Deletion of connexin45 in mouse retinal neurons disrupts the rod/cone signaling pathway between AII amacrine and ON cone bipolar cells and leads to impaired visual transmission. *J Neurosci* 25(3):566–576.
40. Li S, et al. (2005) Requirement for serum response factor for skeletal muscle growth and maturation revealed by tissue-specific gene deletion in mice. *Proc Natl Acad Sci USA* 102(4):1082–1087.